

國立清華大學

碩士論文

我的論文標題 (中文)

My thesis title (Chinese)



系 所：物理研究所

學 號：105022511

研 究 生：韓正忻 (Cheng-Hsin Han)

指導教授：徐百嫻 博士 (Prof. Pai-Hsien Jennifer Hsu)

中 華 民 國 一〇七 年 十 二 月



Todo list

■ “Todo List” will hide when set `\setboolean{publish}{true}` in `config.tex`. . . . iii

“Todo List” will hide when set `\setboolean{publish}{true}` in `config.tex`.





我的論文標題 (中文)

摘要

在此寫上你的中文摘要。

關鍵字：關鍵字, 論文, 樣板, 讓我畢業





My thesis title (Chinese)

Abstract

Write your English abstract here.

Keywords: Keyword, Thesis, Template, Graduate me





Acknowledgement

Thanks NCU, and sppmg's L^AT_EX template `_sppmg/tw_thesis_template_????`.





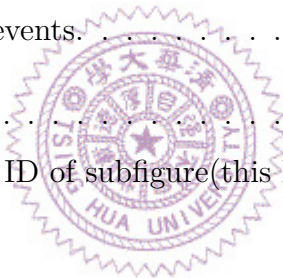
Contents

	page
摘要	v
Abstract	vii
Acknowledgement	ix
Contents	xi
Glossary	xvii
1 Introduction	1
2 The ATLAS detector	3
2.1 Coordinates	3
2.2 Components of ATLAS	3
2.2.1 Inner Detector	5
2.2.2 Calorimeters	5
2.2.3 Muon Spectrometer.....	6
2.2.4 Trigger System.....	6
3 Object Selection and Reconstruction	7
3.1 Jets	7
3.1.1 Small-radius Jets	8
3.1.2 Large-radius Jets	8
3.1.3 Variable-radius Jets.....	8
3.2 Leptons.....	9
3.2.1 Electrons.....	9
3.2.2 Muons.....	10
3.2.3 Taus.....	10

3.3	Missing Transverse Momentum	10
3.4	Overlap Removal	12
4	Event Selection	13
4.1	Signal Region	14
4.2	Control Region	15
4.2.1	1-muon Control Region	16
4.2.2	2-lepton Control Region	16
5	Chapter name(demo)	19
5.1	Section name	19
5.1.1	Subsection name	19
6	Test demo	21
7	figure	23
7.1	Insert single figure(by sppmg's tool)	23
7.2	Insert figures	23
8	Table	25
8.1	Simple table	25
8.2	Auto break line table	25
A	List of device	27
B	Solutions	29
B.1	The solution	29
C	Code	31
C.1	C	31
C.2	Matlab	31
C.3	IDL	31

List of Figures

	page
2.1 short caption	4
2.2 short caption	4
4.1 short caption	13
4.2 The Feynamn diagram of the main background events of the Z' -2HDM model. From left to right, (a) shows the $t\bar{t}$; (b) shows the W +jets events; (c) shows the Z +jets events.	16
7.1 short caption	23
7.2 caption, use “(b)” get ID of subfigure(this ID is Debian) in caption	24





List of Tables

	page
3.1 The summarization of the jet selection and reconstruction.	7
3.2 The summarization of lepton selection and reconstruction. The rightmost column are the requirements for the reconstructed small-R jet that decays from a τ -lepton candidate.	9
4.1 placeholder	14
4.2 placeholder	17
8.1 Solution	25
A.1 List of device	27
B.1 The solution	29





Glossary

Use table for symbol list. You can also use package “nomencl” (simple) or “glossaries” (powerful). see packages document or my tutorial (but it’s Chinese).

Glossary

VIM : The best guy’s editor
Emacs : The God’s editor
CTAN : Comprehensive TeX Archive Network, ctan.org





Chapter 1

Introduction

(You can copy “chapter_template.tex” or “chapter_template_demo.tex” to create new sub-file(chapter).)

Write your Introduction here. eg,

I don't want my chaste thesis impinge by M\$. But \LaTeX is little hard.





Chapter 2

The ATLAS detector

2.1 Coordinates

The ATLAS (**A** **T**oroidal **L**HC **A**pparatu**S**) experiment is one of the seven detector in Large Hadron Collider (LHC) at CERN (European Organization for Nuclear Research). Its cylindrical symmetry and end caps covers nearly 4π in solid angle.

A coordinate system is used to describe every recorded signals nearby. The origin is set at the center of the detector, or the interaction point (IP). The x-axis points toward the center of the LHC ring; the y-axis points vertically upward; the z-axis points along one of the beam pipe direction such that a right-handed coordinate sysetem is created.

A modified version of cylindrical coordinate is more commonly used in the experiment. The pseudorapidity $\eta \equiv -\ln \tan(\theta/2)$, in which θ is the polar angle in cylindrical coordinate, is used to decribe the angle between the z-axis and the direction of interest. (r, ϕ) is the same system to describe the tranverse plane, with ϕ being the azimuthal angle. In addition, the cone size variable, which is used in object selection and reconstruction, is defined as $\Delta R \equiv \sqrt{(\Delta\phi)^2 + (\Delta\eta)^2}$.

2.2 Components of ATLAS

Depending on its function, the components are categorized into four parts - inner detector, calorimeters, muon spectrometer, and the magnetic system. Apart from these, there are three levels of triggers which are designed to reduce the amount of data and also keep the signals of interest. Figure 2.1 shows the schematic positions and 2.2 shows

the side view of each components of ATLAS. The solenoidal magnets surround the inner detector while the toroidal magnets affects the signals in the muon spectrometer. Thses two magnets form the magnetic system. The others consist of smaller layers or components which is described in the following.



Figure 2.1: Schematic plot of the ATLAS detector as well as the positions of its components.



Figure 2.2: Schematic plot of the side view of the ATLAS detector.

2.2.1 Inner Detector

Beginning few centimeters from the IP, the inner detector's main function is to track the trace of charged particles by their interactions with the materials. A 2T magnetic field, which is generated from the solenoidal magnets surrounding the whole inner detector, causes the charged ones to bend. Based on the directions and the curvatures, one can determine their charges and momenta preliminarily. The inner detector comprises three parts - the pixel detector, the semi-conductor tracker (SCT), and the transition radiation tracker (TRT).

Located at the innermost part, the pixel detector contains four layers of modules, which is made up silicon, in the direction perpendicular to the beam. It covers pseudorapidity range $|\eta| < 2.5$ and its proximity to the IP is meant to measure extremely precise trace of the charged particles. Made up of similar material, three disks are at each end cap of the detector.

The semi-conductor tracker, having a similar concept and function to the pixel detector, lies in the middle part of the inner detector. Although having a resemblance to the pixel detector, the SCT is in a long and narrow strip-shape rather than small pixels and covers the perpendicular directions to the beam instead of nearly full coverage. The SCT, which overlays a larger area than the pixel detector does, has more sampled points and thus is of great importance on tracking the transverse directions with roughly the same accuracy compared to the pixel detector.

The outermost component, TRT, includes straw tube trackers and transition radiation detectors. Though its precision in tracking is not as high and its coverage in pseudorapidity, about $|\eta| < 2.0$, is not as wide as those of the other two components, TRT possesses transition radiation detection capability, which is useful for identifying charged particles. Since the lighter particles tend to have higher speed, which generates greater transition radiation, electrons and positrons, the lightest charged particles, would leave strong signals in TRT.

2.2.2 Calorimeters

Outside the solenoidal magnet, which envelops the inner detector, are the calorimeters. By absorbing the particles, the calorimeters measure the energies of them. Two layers of

components compose the calorimeter systems, the inner electromagnetic (EM) calorimeter and the outer hadronic calorimeter.

As its name suggests, the EM calorimeter absorbs energies from particles that interact electromagnetically, including photons and charged particles. A pseudorapidity of range $|\eta| < 3.2$, which includes the barrel and end cap, is covered by high-granularity lead/liquid argon(LAr) EM calorimeter. In addition, a LAr persampler which is meant to correct the energy loss in materials of the calorimeters covers $|\eta| < 1.8$. For the forward region, which has the range $3.1 < |\eta| < 4.9$, a LAr EM calorimeter with copper is also deployed.

Hadronic calorimeter, although it is less precise in both energy magnitude and localization than EM calorimeter, absorbs energies from the particles that interact via strong force. Hadrons, which is identified as jets, and τ leptons, which mainly decay hadronically, are the targeted particles of hadronic calorimeter. Steel/scintillator-tile covering $|\eta| < 1.7$, two copper/LAr end cap calorimeters overlaying $1.5 < |\eta| < 3.2$, and a forward-regional ($3.1 < |\eta| < 4.9$) tungsten absorbers constitute the hadronic calorimeter.

2.2.3 Muon Spectrometer

Muon spectrometer, which is meant to provide more precise measurement of muon momenta and tracks, surrounds the calorimeters. Due to the fact that few particles rather than muons passes through it, muon spectrometer also has a function of identifying the muons. A magnetic field, provided by three toroidal magnets and thus is not uniform, creates a curve in muon tracks, which can be made use of measuring the momenta. Detectors with triggers provide the identification and momenta measurements of the muons within the range $|\eta| < 2.4$; over a thousand precision tracking chambers covering $|\eta| < 2.7$ serve the muon spatial measurements.

2.2.4 Trigger System

A trigger is a set of device which sets thresholds on some physical quantities such as momenta and positions. If the threshold of one event is met, one keeps it; otherwise one abandons it. The ATLAS triggers consist of three levels. The first level is hardware based while the other two are software based. From roughly 1 billion events per second, these three triggers combined select about few hundreds interesting. Namely, the interaction rate is reduced from 1 GHz to few hundreds Hz.

Chapter 3

Object Selection and Reconstruction

Signals recorded in the ATLAS detector are categorized or reconstructed as physical objects, which could be further used in the analyses. Besides the head-to-head, or hard-scattered, events which have high transverse momentum, or p_T , there are also additional collisions with lower p_T . These are referred to as the pile-up events, which one often wants to exclude in the analyses. The reconstruction and definition of objects used in this study are listed in the following.



3.1 Jets

Jets are the reconstruction of collimated bunches of hadrons. In ATLAS experiment, the anti- k_T algorithm is usually used to recombine hadrons into cone-sized shapes. In short, the anti- k_T algorithm makes use of p_T of each given entities and reconstructs jets whose R is the given radius parameter and which center on hard-scattered particles. How the jets is reconstructed and defined in this study is tabulated in table.3.1 and explained as follows.

Table 3.1: The summarization of the jet selection and reconstruction.

type	(<i>central</i>) small-R jets	(<i>forward</i>) small-R jets	large-R jets	VR track jets
p_T (GeV)	> 20	> 30	> 200	> 0.5
$ \eta $	$(0, 2.5)$	$(2.5, 4.5)$	$(0, 2.0)$	$(0, 2.5)$
R	0.4		1.0	$\rho/p_T \in (0.02, 0.4)$ with $\rho = 30$ GeV
additional	if $ \eta < 2.4$ then $p_T < 60$ GeV	-		$ z_0 \sin(\theta) < 3$ mm

3.1.1 Small-radius Jets

Using the anti- k_T algorithm with a radius parameter of 0.4, small-radius, or small-R, jets can be reconstructed from the energy deposits in the calorimeter. Small-R jets are further categorized into two types, the central jets and the forward jets. Those jets whose $|\eta| < 2.5$ are required to have $p_T > 20$ GeV in order to be identified as the former; other jets with $2.5 < |\eta| < 4.5$ are referred to as the latter and a threshold of $p_T > 30$ GeV is required. For jets in $|\eta| < 2.4$, an additional threshold of $p_T < 60$ GeV is required, and, to further suppress jets from the pile-up interactions, they are required to be originated from the reconstructed location of the collision, or the primary vertex. In addition, jets containing b-quark are referred to as b-jets; the method used to identify them as b-jets are called b-tagging. Because b-quarks have a relative longer lifetime compared to other particles, they would emit from a secondary vertex rather than the primary one, which can be made use of to perform the b-tagging. A working point of 77% on average for the b-tagging efficiency is used in this analysis.

3.1.2 Large-radius Jets

The large-radius, or large-R, jets are reconstructed via the anti- k_T algorithm with a radius parameter of 1.0. The reconstruction highly depends on the calorimeter and the tracking system. Certain calibration method is applied for the energy deposits in the calorimeter. The calibrated jets have a p_T threshold of 200 GeV and are required to be within the range of $|\eta| < 2.0$.

3.1.3 Variable-radius Jets

The variable-radius (VR) track jets are also reconstructed using the anti- k_T algorithm. Those jets whose p_T does not exceed 0.5 GeV or out of the range of $|\eta| < 2.5$ are not considered. To suppress the pile-up jets, a criteria on the longitudinal impact parameter, $|z_0 \sin(\theta)| < 3$ mm, is required, where z_0 is the point closet to the vertex along the longitudinal axis and θ is the polar angle of the track. The main feature of the VR track jets is that the radius parameter depends on the value of p_T rather than a constant value:

$$R \rightarrow R_{\text{eff}} \approx \frac{\rho}{p_T}, \quad (3.1)$$

in which ρ is set at 30 GeV, which is the optimal value regarding the efficiency for b-tagging. The upper limit and lower limit, R_{\max} and R_{\min} are set at 0.4 and 0.02 in this regard.

3.2 Leptons

Leptons are used to categorized the regions selected in this analysis, which would be covered in the next chapter. Requirements of each flavor are explained in the following and summarized in table.3.2.

Table 3.2: The summarization of lepton selection and reconstruction. The rightmost column are the requirements for the reconstructed small-R jet that decays from a τ -lepton candidate.

flavor	e		μ		τ
categorization	baseline	signal	baseline	signal	-
p_T (GeV)	> 7	> 27	> 7	> 25	> 20
$ \eta $	(0, 2.47)		(0, 2.7)	(0, 2.5)	$(0, 1.37) \cup (1.52, 2.5)$
ID	Loose		Loose (0/2-lepton) Medium (1-muon)		Loose
transverse impact parameter	$d_0/\sigma(d_0) < 5$		$d_0/\sigma(d_0) < 3$		$ d_0 < 1$ mm
$ z_0 \sin(\theta) $ (mm)			< 0.5		< 1.5
Additional			-		one to four track-jets $\Delta\phi(\tau, \cancel{E}_T) < \frac{\pi}{8}$

3.2.1 Electrons

Electron candidates are reconstructed from the energy deposits in EM calorimeter that match a track recorded in the inner detector. In addition, there is a LLH-based algorithm, which further makes use of multivariable analysis (MVA), applied for the electron ID. Three levels of ID operating point, loose, medium and tight, are provided; among them, loose ID is used in this study for the electrons. Moreover, electrons are divided into two groups, the baseline electrons, whose p_T exceed 7 GeV, and the signal electrons, which require a tighter threshold of $p_T > 27$ GeV. All candidates within $|\eta| < 2.47$ are considered. Finally, requirements of the impact parameter are examined, both in the transverse and longitudinal directions. For the former, the relative resolution, which is the fraction of the transverse impact parameter d_0 and its resolution $\sigma(d_0)$, has an upper bound of 5. For

the latter, the value $|z_0 \sin(\theta)| < 0.5$ mm is set.

3.2.2 Muons

Muon candidates, also divided into baseline and signal muons, are reconstructed with high dependence of inner detector and the muon spectrometer. Signal muons, whose p_T exceed 27 GeV, are more likely to leave tracks in the inner detector, and thus shall be found in $|\eta| < 2.5$. For baseline muons, which have a looser p_T threshold of 7 GeV, leaving signals in the inner detector is not required and thus are within $|\eta| < 2.7$, which is the range of the muon spectrometer. On top of that, the impact parameter must be consistent with the the primary vertex. $d_0/\sigma(d_0) < 3$ and $|z_0 \sin(\theta)| < 0.5$ mm are set. Finally, a loose ID is used for the zero-lepton and two-muon channel whilst the one-muon channel makes use of a medium ID for the muons in this analysis. These channels would be covered in the upcoming chapter.

3.2.3 Taus

τ -leptons, whose decay length is few μm , barely reach the ATLAS detector and thus are mainly reconstructed from their decay products. Due to the fact that most of the τ -leptons decay into hadrons, the τ -lepton candidates are reconstructed from jets. The transverse impact parameter, $|d_0| < 1$ mm, and the longitudinal one, $|z_0 \sin(\theta)| < 1.5$ mm, are set for the jet tracks and the τ vertex. The threshold on the p_T of the jets is set at 20 GeV; the range of $|\eta| < 2.5$, excluding $1.37 < |\eta| < 1.52$, which is the region between the barrel and the forward region, or the crack region, is also required. Furthermore, the ID is built on a boosted decision tree (BDT) that makes use of the information from the tracks and the calorimeter. The loose working point on the τ -leptons is used. Finally, the small-R jet is required to contain one to four track-jets and within a range of $\Delta\phi < \frac{\pi}{8}$ with the missing transverse energy (MET, E_T^{miss} or \cancel{E}_T) in order to suppress the W-boson-decayed τ -leptons.

3.3 Missing Transverse Momentum

The missing transverse momentum is the imbalance in p_T of the reconstructed objects. Thus, it can be reconstructed as the negative vector transverse momentum sum. This

includes the hard-scattered objects and the soft term. The momentum of hard-scattered reconstructed particles construct the former. As for the soft term, tracks that are not associated to any reconstructed hard objects are considered. The vetoed leptons, which are the leptons that needs to removed from the analysis in some channels, which would be covered in the next chapter, also count as the soft term. Jets that failed the selection of small-R jets also contributes the soft term, with the p_T threshold on the forward small-R jet being modified to 20 GeV. The absolute value of the missing transverse momentum is denoted as E_T^{miss} (or \cancel{E}_T).

An estimation variable E_T^{miss} significance, S , is used to check the genuinity in whether E_T^{miss} comes from undetectable particles instead of mismeasurements or any inefficiencies. There are two types of E_T^{miss} significance, the event-based one and the object-based one. The former one is the ratio of the E_T^{miss} and the square root of the transverse momentum of hard-scattered particles, H_T , i.e.,



$$S_{\text{event}} = \frac{E_T^{\text{miss}}}{\sqrt{H_T}}, \quad (3.2)$$

where

$$H_T = \Sigma p_T^\mu + \Sigma p_T^e + \Sigma p_T^\gamma + \Sigma p_T^\tau + p_T^{\text{jets}}. \quad (3.3)$$

If the soft term contributes little in the transverse momentum, the value of H_T would be approximately that of E_T^{miss} , and thus the value of E_T^{miss} significance tends to be small. It would be used in the background estimation mainly and would be used as cut in the next chapter.

The other significance value, the object-based one, is a log-likelihood ratio value. It is used to test the hypothesis that the total momentum of the invisible particle is zero against the hypothesis that it is not. In short, if the value of the object-based significance, S_{object} which is non-negative, is close to zero, then it implies high possibilities that E_T^{miss} does not come from the invisible particles; if the value is large, then it implies a possibility of existing invisible particles.

3.4 Overlap Removal

Object ambiguities happen when objects match multiple reconstruction criteria. In the following listed specific steps of object reconstruction that are required to solve the problem.

1. If two electron candidates share the same track, remove the one with lower p_T .
2. If a τ -lepton candidate lies within $\Delta R = 0.2$ of an electron or muon, it is removed.
3. Reject the electron candidates whose track is shared with a muon candidate.
4. Small-R jets are removed if they are within $\Delta R = 0.2$ of an electron.
5. Remove the electrons that are within $\Delta R = \min(0.4, 0.04 + 10\text{GeV}/p_T^{\text{electron}})$ of a small-R jet.
6. If the separation between a small-R jet and a muon is within $\Delta R = 0.2$, the small-R jet is removed provided that it has fewer than three tracks or that the muon p_T is greater than 50% of the jet p_T and is greater than 70% of the p_T sum of the tracks associated to the jets.
7. Remove the muons that are within $\Delta R = \min(0.4, 0.04 + 10\text{GeV}/p_T^{\text{muon}})$ of a small-R jet.
8. Large-R jets whose track is within $\Delta R = 0.1$ to that of an electron are removed.

Chapter 4

Event Selection

A number of selection is applied on the events in this study. Because the final state of the Z' -2HDM model contains no leptons (see fig. 4.1), one can define this zero-lepton region as the signal region (SR). However, there are other processes having the same final products as that of this model, which is recognized as the background. To further estimate the amount of the background events, one analyzes other processes that are similar to the background. These processes are called the control region (CR). Both SR and CR are discussed in this chapter. Some comparisons and characteristic selections of SR and CRs are summarized in table 4.1.

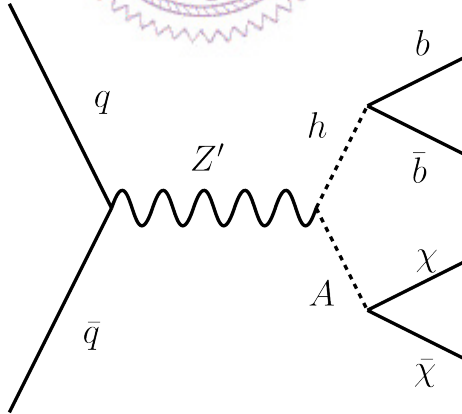


Figure 4.1: The Feynman diagram of the Z' -2HDM model.

Table 4.1: placeholder

region	signal region	1-muon control region	2-lepton control region
lepton selection	no loose leptons	one signal muon no baseline electrons	two baseline muons or electrons one of them being signal
(proxy) missing transverse momentum	E_T^{miss}	$E_T^{\text{miss}, \text{no}\mu} = E_T^{\text{miss}} + p_T^\mu$	p_T^{ll}
E_T^{miss} significance selection	$S_{\text{object}} > 16$	-	$S_{\text{event}} < 3.5 \text{ GeV}^{\frac{1}{2}}$
additional	-	-	$83(99) \text{ GeV} < m_{\text{ee}(\mu\mu)} < 99(106) \text{ GeV}$ opposite muon charge

4.1 Signal Region

First, no baseline leptons candidates, including the τ -leptons, are considered. The value of E_T^{miss} is required to be at least 150 GeV. Multijet backgrounds may pass the selection criteria. To further suppress this background, one adds two selections. The first one requires the azimuthal angle between E_T^{miss} and any of the three highest- p_T jets ($\min(\Delta\phi(E_T^{\text{miss}}, \text{jet}))$) greater than 20° . The forward jets are only considered if the number of central jets is less than 3. The other selection requires the azimuthal angle between E_T^{miss} and p_T^{miss} smaller than 90° , where p_T^{miss} is the negative sum of object momentum measured by the inner detector.

After these selections, one divides these events into two regions based on the value of E_T^{miss} . Those whose E_T^{miss} is smaller than 500 GeV are defined as the resolved region, whilst the merged region contains those events with $E_T^{\text{miss}} > 500$ GeV. The resolved region are further divided into three regions, whose E_T^{miss} are within (150, 200], (200, 350], and (350, 500]. Different sets of selections are applied in these two regions and tabulated in table 4.2.

For the resolved region, the events are required to have at least two small-R jets, which is the reason of the naming of this region. In these jets, exactly two b-tagged jets are also required. The p_T of one of the jets has to exceed 45 GeV. For the events with two (three or more) jets, the scalar sum of the p_T of the highest two (three) jets is also required to be at least 120 (150) GeV. A requirement of $S_{\text{object}} > 16$ is also applies. To further suppress the multijet backgrounds, a selection on the separation are required. Due to the conservation of the momentum, one expects the tracks of the E_T^{miss} and the Higgs candidate are back-to-back. The azimuthal angle between E_T^{miss} and the Higgs candidate

is required to be greater than 120° . The azimuthal angle between the two jets from the Higgs candidate ($\Delta\phi(\text{jet}_1, \text{jet}_2)$) tends to be large in multijet background events because of the topology. Thus, it is required to be smaller than 140° in this study. Furthermore, in order to reject $t\bar{t}$ background events, two more selections are added. One of them is $\Delta R(\text{jet}_1, \text{jet}_2) < 1.8$. The scalar sum of the first three highest p_T of the jets is required to be greater than 63% of the scalar sum of all jets is considered as the other one. At last, one adds a Higgs mass window selection on the two b-tagged jets, $50 \text{ GeV} < m_{jj} < 280 \text{ GeV}$.

As for the merged region, the events which contains at least one large-R jets are considered, which is the reason of the name "merged". The large-R (VR track) jet with the highest p_T are referred to as the leading large-R (VR track) jet. Two leading VR track jets associated with the leading large-R jet are required be to b-tagged. Events with any VR track jets outside the large-R jets are rejected. To suppress the $t\bar{t}$ background events, the value of p_T of the leading large-R jet is required to exceed 43% of the scalar sum of the p_T of the leading large-R jets and all small-R jets. Finally, the invariant mass of the large-R jet is also required to be within a Higgs mass window, $50 \text{ GeV} < m_J < 270 \text{ GeV}$.

4.2 Control Region

Events containing leptons are used to define the CRs. One makes use of the CRs to estimate the main backgrounds of the Z' -2HDM model shown in fig. 4.1. These main backgrounds are shown in 4.2. Based on the number of leptons, the background events can be further categorized into two CRs. The $t\bar{t}$ and W +jets production define the 1-muon CR. The 2-lepton CR contains the Z -jets events.

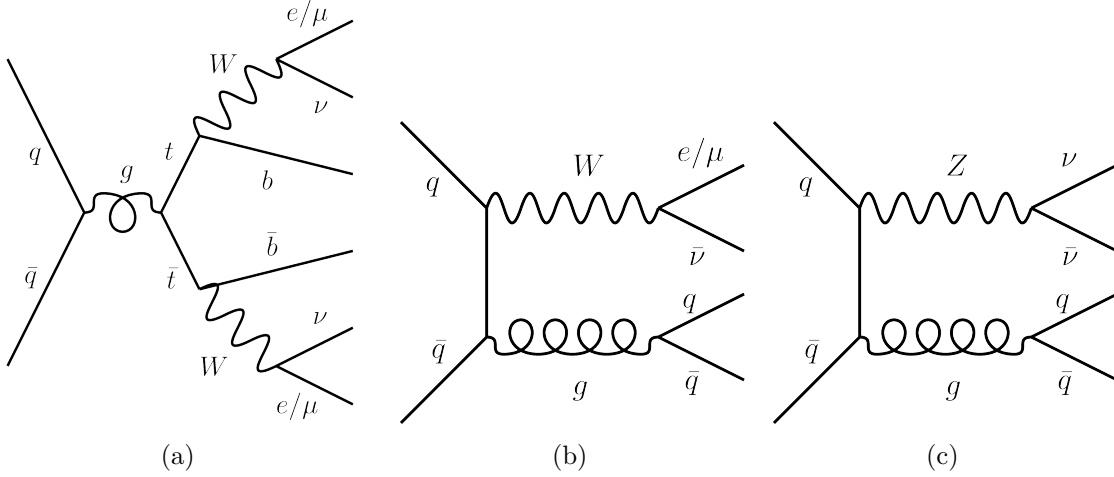


Figure 4.2: The Feynman diagram of the main background events of the Z'-2HDM model. From left to right, (a) shows the $t\bar{t}$; (b) shows the W+jets events; (c) shows the Z+jets events.

4.2.1 1-muon Control Region

Although there are leptons in figure 4.2 (a) and (b), these events become the backgrounds because of misidentification or missed detections. As a result, the misidentified or undetected leptons would contribute to the E_T^{miss} . The 1-muon CR is made use of estimating the backgrounds of these $t\bar{t}$ and W+jets events.

Because of the relatively higher fake rate of identification, single electron events are not considered in this background estimation. Therefore, no baseline electrons and exactly one signal muon are required. To mimic how these background events in SR behave, a "proxy" missing transverse momentum is defined as the sum of E_T^{miss} and the transverse momenta of the muon, or $E_T^{\text{miss}, \text{no}\mu}$. The resolved and merged region are also defined using the threshold of 500 GeV on $E_T^{\text{miss}, \text{no}\mu}$. Other selections are the same as those mentioned in section 4.1 except the S_{object} selection in the resolved region.

4.2.2 2-lepton Control Region

The neutrinos in figure 4.2 (c) cannot be detected and thus are part of the contributions to the E_T^{miss} . The 2-lepton CR serves as the estimation of this background.

Two same-flavor leptons are required first. For both two-electron or two-muon cases, one lepton is required to be the signal one while the other has to pass the criteria of the baseline one. Additional requirement for the two-muon case is to have opposite charge. In

order to make sure that the lepton pair truly decay from the Z boson candidate, a dilepton mass window is applied. The requirement on invariant mass of the two-electron (muon) system is $83 \text{ GeV} < m_{ee} < 99 \text{ GeV}$ ($71 \text{ GeV} < m_{\mu\mu} < 106 \text{ GeV}$). The "proxy" missing transverse momentum is the absolute value of the sum of the transverse momentum of the two-leptons, or p_T^{ll} . One makes use of p_T^{ll} to define the resolved merged region based on the 500 GeV boundary. Those selections stated in section 4.1 except the S_{object} selection in the resolved region are applied. Apart from that, in order to reduce the $t\bar{t}$ and single top background in this CR, the S_{event} is required to be less than $3.5 \text{ GeV}^{\frac{1}{2}}$.

Table 4.2: placeholder

resolved	merged
τ -veto	
$\min(\Delta\phi(E_T^{\text{miss}}, \text{jet})) > 20^\circ$	





Chapter 5

Chapter name(demo)

Content of chapter
Content Content Content.

5.1 Section name

Content of section
Content Content Content



5.1.1 Subsection name

Content of subsection
Content Content Content

5.1.1.1 Subsubsection name

Content of subsubsection
Content Content Content

5.1.1.1.1 Paragraph name Content of paragraph
Content Content Content

Subparagraph name Content of subparagraph
Content Content Content



Chapter 6

Test demo

First line. (next line in \LaTeX)still first line.
Second line.





Chapter 7

figure

7.1 Insert single figure(by sppmg's tool)

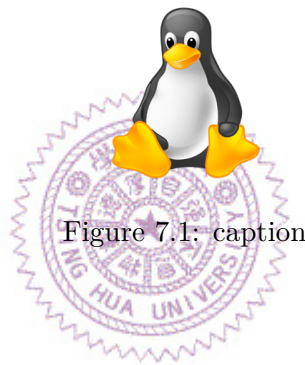


Figure 7.1: caption

7.2 Insert figures

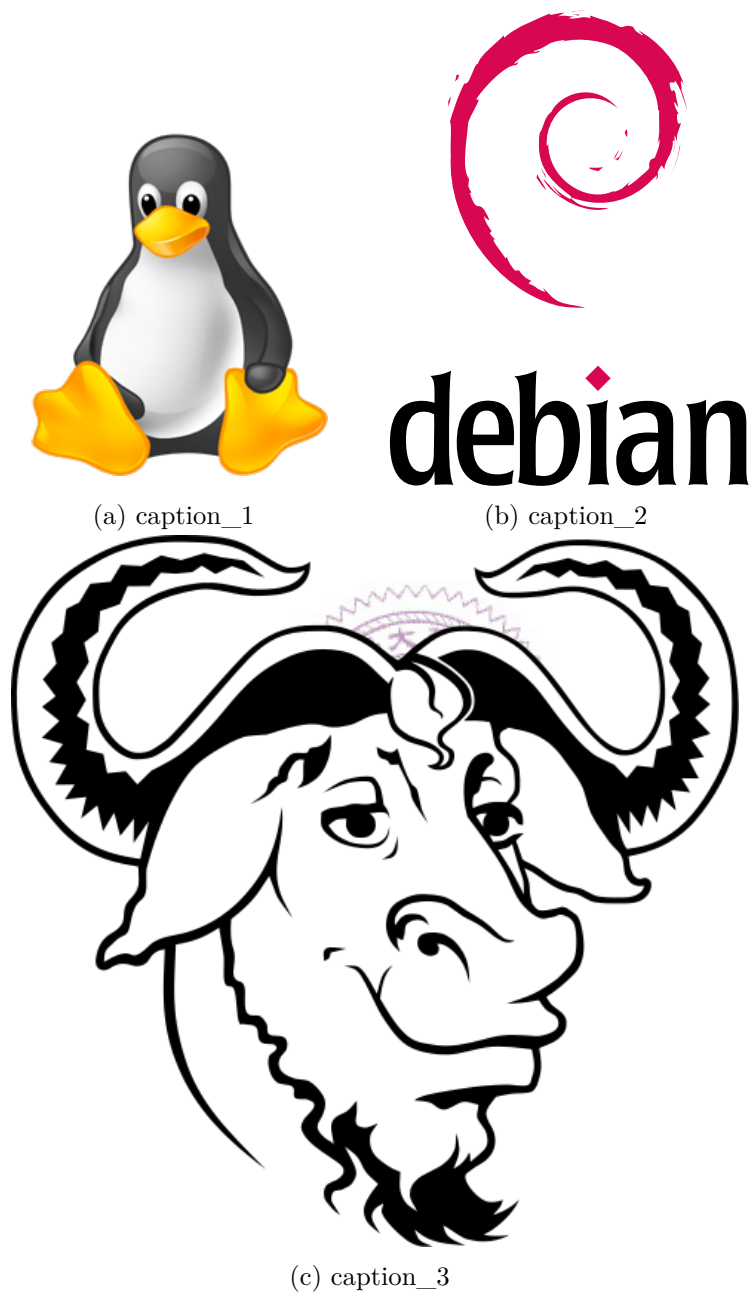


Figure 7.2: caption, use “(b)” get ID of subfigure(this ID is Debian) in caption

Chapter 8

Table

8.1 Simple table

Table 8.1: Solution

Component	Concentration(mM)
CaCl ₂	118.0

8.2 Auto break line table

short	short short
long	long long long long long long long long long



Appendix A

List of device

Table A.1: List of device

device	Model	Description
Linux	Debian 9	Best of best of best OS
Windows	10	Best of Best tool to prevent the aging of brain.





Appendix B

Solutions

B.1 The solution

Table B.1: The solution

Component	Concentration(mM)
NaCl	1.0
CaCl ₂	2.0
NaCl	1.0
CaCl ₂	2.0




Appendix C

Code

C.1 C

Code C.1: hello_world_c.c

```
1 #include <stdio.h>
2 main()
3 {
4     printf("hello, world\n");
5 }
```



C.2 Matlab

Code C.2: hello_world_matlab.m

```
1 fprintf('hello, world\n');
```

C.3 IDL

Code C.3: hello_world_idl.pro

```
1 print,"hello, world"
2
3 end
```